Geodesy and Geodynamics 10 (2019) 430–438

Contents lists available at ScienceDirect

Geodesy and Geodynamics

journal homepage: http://www.keaipublishing.com/geog

Hydrological mass variations in the Nile River Basin from GRACE and hydrological models

Mostafa Abd-Elbaky [a, b, c], Shuanggen Jin [a, *]

[a] Shanghai Astronomical Observatory, Chinese Academy of Sciences, Shanghai, 200030, China
[b] University of Chinese Academy of Sciences, Beijing 100084, China
[c] Civil Engineering Department, Faculty of Engineering, Minia University, Minia, 6111, Egypt

ARTICLE INFO

Article history:
Received 23 March 2018
Accepted 29 July 2019
Available online 7 August 2019

Keywords:
Terrestrial water storage
Nile River Basin
GRACE
TRMM
Climate change

ABSTRACT

Terrestrial water storage (TWS) change is a key component of the global water cycle and hydrologic cycle. Therefore, it is of significance to quantify TWS variations at large scale and understand how the climate changes affect in the water systems, particularly in the Nile River Basin. In this study, TWS variations in the Nile River Basin are estimated and investigated from January 2003 to August 2016 by using the Gravity Recovery and Climate Experiment (GRACE). Also, the Global Land Data Assimilation System (GLDAS) and Tropical Rainfall Measuring Mission (TRMM) are used to understand the causes of the TWS variations in the Nile River Basin (NRB). The peak of precipitation has happened in July and August. After one month the appearance of the influence of precipitation on soil moisture is clear. On the other hand, after two months the same effect of precipitation in TWS is clear. While the peak of soil moisture has occurred in August and September, the maximum of TWS has observed in September and October. The maximum annual TWS from GRACE measurements is 42.66 mm in NRB during September–November (autumn), and its minimum is −33.77 mm during March–May (spring). Also, the maximum annual soil moisture is 25.22 mm in NRB during September–November (autumn), and its minimum is −23.34 mm during March–May (spring) while the peak precipitation is 100.11 mm during June–August (summer) and its minimum is 14.62 mm during December–February (winter). The trend of TWS variations in NRB is 0.04 mm/yr from GRACE. Furthermore, the TWS variations are mainly dominated by the soil moisture in the Nile River Basin with the correlation coefficient of 0.88. In addition, the correlation factor between the non-seasonal TWS and ScPDSI is 0.60, indicating that GRACE-derived TWS well capture the most severe droughts occurred in 2006 and 2011.

© 2019 Institute of Seismology, China Earthquake Administration, etc. Production and hosting by Elsevier B.V. on behalf of KeAi Communications Co., Ltd. This is an open access article under the CC BY-NC-ND license (http://creativecommons.org/licenses/by-nc-nd/4.0/).

1. Introduction

The Nile River is of great importance in the economies and agriculture of the Nile River Basin (NRB) countries. For example, farmers in all the NRB countries rely on its water to irrigate their crops. The Nile River plays a key role in the sustenance of the people of the NRB. Therefore, monitoring of water changes in the NRB is essential. The terrestrial water storage change is a major role in the water cycle and hydrologic cycle [1]. Unfortunately, the in situ observations are very sparse globally, particularly in Africa [2]. Moreover, traditional measurements have some limitations due to high costs and low resolution. GRACE satellite mission is used to monitor the Earth's gravity field. The Earth's mass redistributions have measured with a spatial resolution of few hundred kilometers and monthly temporal resolution. GRACE provides monthly gravitational field data which can infer the trends in surface-mass anomalies. TWS includes groundwater, soil moisture, surface water bodies (lakes, rivers, and reservoirs), glaciers, snow water equivalent, and canopy water storage [3,4].

Global climate change affects water resources around the world. Therefore, it is helpful to understand how the climate

* Corresponding author.
E-mail addresses: mstabdelbaky@gmail.com, mostafa.tony@mu.edu.eg (M. Abd-Elbaky), sgjin@shao.ac.cn, sg.jin@yahoo.com (S. Jin).

Peer review under responsibility of Institute of Seismology, China Earthquake Administration.

Production and Hosting by Elsevier on behalf of KeAi

https://doi.org/10.1016/j.geog.2019.07.004
1674-9847/© 2019 Institute of Seismology, China Earthquake Administration, etc. Production and hosting by Elsevier B.V. on behalf of KeAi Communications Co., Ltd. This is an open access article under the CC BY-NC-ND license (http://creativecommons.org/licenses/by-nc-nd/4.0/).

change impacts on water systems. Climatic extremes (e.g. drought) are normal climatic occurrences in Africa. Awange et al. (2007) described how extensive droughts are a regular feature in parts of East Africa in the last few decades [5]. For Africa basin, the strong signal of annual TWS amplitude has found in Zambezi and Okavango River basins in south-central Africa. But, Volta River Basin in western Africa has maximum annual amplitude of TWS detected by GRACE. Therefore, Hassan et al. (2016) inferred that TWS in these parts has been mainly dominated by rainfall as well as soil moisture content [6]. The trend of TWS shows seasonal (30 ± 6 mm of equivalent water thickness). Whereas, the rainfall contributed three times the peak water storage after anomalously rainy seasons, in early 2003 and 2005 in Congo Basin in Africa [7]. Also, combining storage deficits with event duration can calculate drought severity [8].

In this paper, the influence of the climate change on TWS is investigated in the NRB. In section 2, the processing methods are illustrated by GRACE and GLDAS. In section 3, the results and analyses of TWS variations are presented. In section 4, the correlations between TWS and climate change are discussed as well as the impact of climate change on TWS. Finally, the conclusions are given in section 5.

2. Method and data

The Nile River is located in the northeastern part of Africa, which is recognized as the world's longest river with a length of about 6825 km [9]. Moreover, the NRB extends from 5° South to 31° North with a covering area of 3.4 million Km^2 across 11 countries (Fig. 1).

2.1. TWS from GRACE

GRACE time-variable monthly gravity solutions are used to estimate the large-scale mass change [10]. The change in water storage from GRACE is a perfect fit for a water budget studies [11–14]. GRACE RL05 level-2 time-variable gravity solutions have been used from the Center for Space Research (CSR), University of Texas at Austin, which is one of the three data centers. The 149 monthly gravity solutions cover the period from January 2003 to August 2016. The fully normalized spherical harmonic coefficients till degree and order 60 have been used. According to noise and some errors in GRACE gravity solutions, especially in the short wavelength (high degree) spherical harmonic coefficients, the correlated error filter has been used [15,16]. For a given spherical harmonic order (6 and above), least squares fit is used to the fit to the odd and even coefficient pairs and remove a polynomial (of order 5). This processing step is denoted as P5M6. Then, 400 km Gaussian low-pass filter smoothing has been applied. The new spherical harmonic coefficients are used to compute the terrestrial water storage by removing the mean value of the all monthly solutions [15,17]. The new spherical harmonic coefficients are given by:

$$\begin{Bmatrix} \Delta\overline{C}_{lm} \\ \Delta\overline{S}_{lm} \end{Bmatrix} = \begin{Bmatrix} \overline{C}_{lm} - \left(\sum_{i=1}^{n} (\overline{C}_{lm})_i / n \right) \\ \overline{S}_{lm} - \left(\sum_{i=1}^{n} (\overline{S}_{lm})_i / n \right) \end{Bmatrix} \quad (1)$$

where $\Delta\overline{C}_{lm}$ and $\Delta\overline{S}_{lm}$ are the changes in the fully normalized spherical harmonic coefficients, $\overline{C}_{lm}$ and $\overline{S}_{lm}$ are the fully normalized spherical harmonic coefficients, l and m are the degree and order respectively, and n is the number of the months. The degree 2 zonal term Stokes coefficient $C_{2,0}$ is replaced with the Stokes coefficients estimated from SLR [18] and the degree 1 has been added [19,20]. Thus the Terrestrial Water Storage (TWS) can be computed as an equivalent water layer thickness change on grid by [21]:

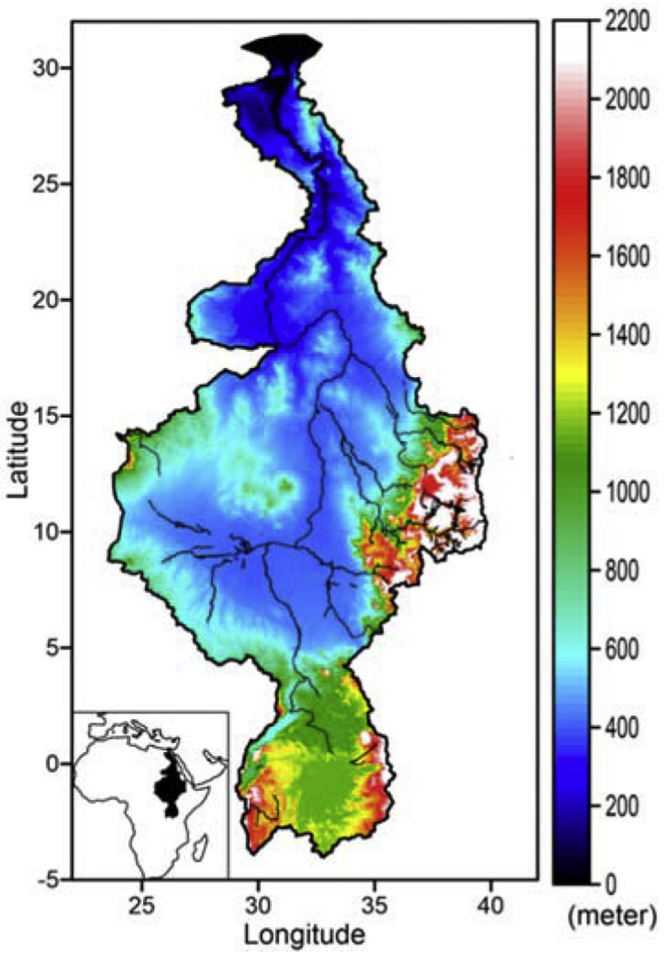

Fig. 1. Nile River Basin in Africa.

$$\Delta\eta(\theta,\phi) = \frac{a\,\rho_{\text{ave}}}{3\,\rho_{\text{water}}} \sum_{l=0}^{\infty} \sum_{m=0}^{l} \frac{2l+1}{1+K_l} \overline{P}_{lm} \cos\theta \left(\Delta\overline{C}_{lm} \cos m\phi + \Delta\overline{S}_{lm} \sin m\phi \right) \quad (2)$$

where θ and ϕ are colatitude and longitude respectively, a is the radius of the Earth (= 6378136.300 m), ρ_{ave} is the average density of the Earth (= 5517 kg/m^3), ρ_{water} is the density of water (assumed throughout this paper to be 1000 kg/m^3), K_l is the load Love number of degree l, and $\overline{P}_{lm}$ is the fully normalized associated Legendre functions.

2.2. TWS from GLDAS

GLDAS is one of the better hydrological models representing the spatial and temporal variability of land water at a global scale. GLDAS is generating a series of land surface state and flux products simulated by four land surface models (CLM, Mosaic, NOAH and VIC). In this paper, NOAH land surface model [22] has used to estimate the TWS. NOAH contains the precipitation data from a spatially and temporally downscaled version of the NOAA Climate Prediction Center's Merged Analysis of Precipitation and the

monthly average soil moisture (4 layers, 2 m column depth) and snow water equivalent were computed from 1979 to present. Meanwhile, the groundwater is not modeled by GLDAS. In this paper, the monthly data with a spatial resolution 1.0° × 1.0° from NOAH are used. TWS computed as the summation of soil moisture in all layers, accumulated snow, and plant canopy surface water [23].

$$TWS_{\mathrm{GLDAS}} = \sum_{i=1}^{n} SM_i + SWE + CWS \tag{3}$$

where SM is soil moisture, n is the number of the layers, SWE is snow water equivalent, and CWS is canopy surface water. TWS from GLDAS has represented in a spherical harmonics expansion to degree and order 60. Spherical harmonics coefficients have computed using Gauss numerical integration method. The analytical function $f(\theta,\phi)$ defined on the unit sphere $(0 \le \theta \le \pi$ and $0 \le \phi \le 2\pi)$. $f(\theta,\phi)$ can be expanded in series of surface spherical harmonics [24].

$$f(\theta,\phi) = \sum_{n=0}^{\infty} \sum_{m=0}^{n} \overline{P}_{nm}(\cos\theta)\left[\overline{C}_{nm}\cos m\phi + \overline{S}_{nm}\sin m\phi\right] \tag{4}$$

where $\overline{C}_{nm}$ and $\overline{S}_{nm}$ are the fully normalized spherical harmonic coefficients and $\overline{P}_{nm}$ is the fully normalized associated Legendre functions. The fully normalized harmonic coefficients are orthogonal. Then, the spherical harmonics coefficients achieve the orthogonality relations. As a consequence of the orthogonality, the fully normalized harmonic coefficients can be written as [25]:

$$\begin{Bmatrix} \overline{C}_{nm} \\ \overline{S}_{nm} \end{Bmatrix} = \frac{1}{4\pi} \iint_{\sigma} f(\theta,\phi) \begin{Bmatrix} \overline{R}_{nm}(\theta,\phi) \\ \overline{Q}_{nm}(\theta,\phi) \end{Bmatrix} d\sigma \tag{5}$$

Indeed, Eq. (5) cannot be used to compute the spherical harmonics coefficients because the analytical function $f(\theta,\phi)$ is not available. A finite set of noisy measurements $f(\theta_i,\phi_i)$ covers the whole sphere may be available. Discretizing Eq. (5) on an equal angular grid covering the whole sphere gives the following numerical quadratures formula.

$$\begin{Bmatrix} \widehat{C}_{nm} \\ \widehat{S}_{nm} \end{Bmatrix} = \frac{1}{4\pi} \sum_{i=0}^{N-1} \sum_{j=0}^{2N-1} f(\theta_i,\phi_i)\overline{P}_{nm}(\cos\theta_i) \begin{Bmatrix} \cos m\phi_i \\ \sin m\phi_i \end{Bmatrix} \Delta_{ij} \tag{6}$$

where $\widehat{C}_{nm}$ and $\widehat{S}_{nm}$ are the estimates of $\overline{C}_{nm}$ and $\overline{S}_{nm}$ respectively, N is the number of grids in the latitude direction, and Δ_{ij} is indicates the segment area. The segment area can be computed as:

$$\Delta_{ij} = 2\,\Delta\phi \sin\left(\frac{\Delta\theta}{2}\right)\cos\theta_i \tag{7}$$

P5M6 has applied on the estimated spherical harmonics coefficients. Then, Gaussian low-pass filter smoothing has been applied. The spherical harmonics coefficients for degree 1 and degree 2 were set as they are for the GRACE processing. The new spherical harmonic coefficients have used to compute the terrestrial water storage. Finally, the TWS is estimated from GLDAS on a global 1.0° × 1.0° grid. The annual amplitude and trend of TWS in the NRB from GRACE and GLDAS in the period of study is shown in Fig. 2. The tropical region shows a large seasonal variation with the maximum annual amplitude of 126 mm and maximum trend is 11 mm/yr. It is clear that GRACE gives a higher value than GLDAS.

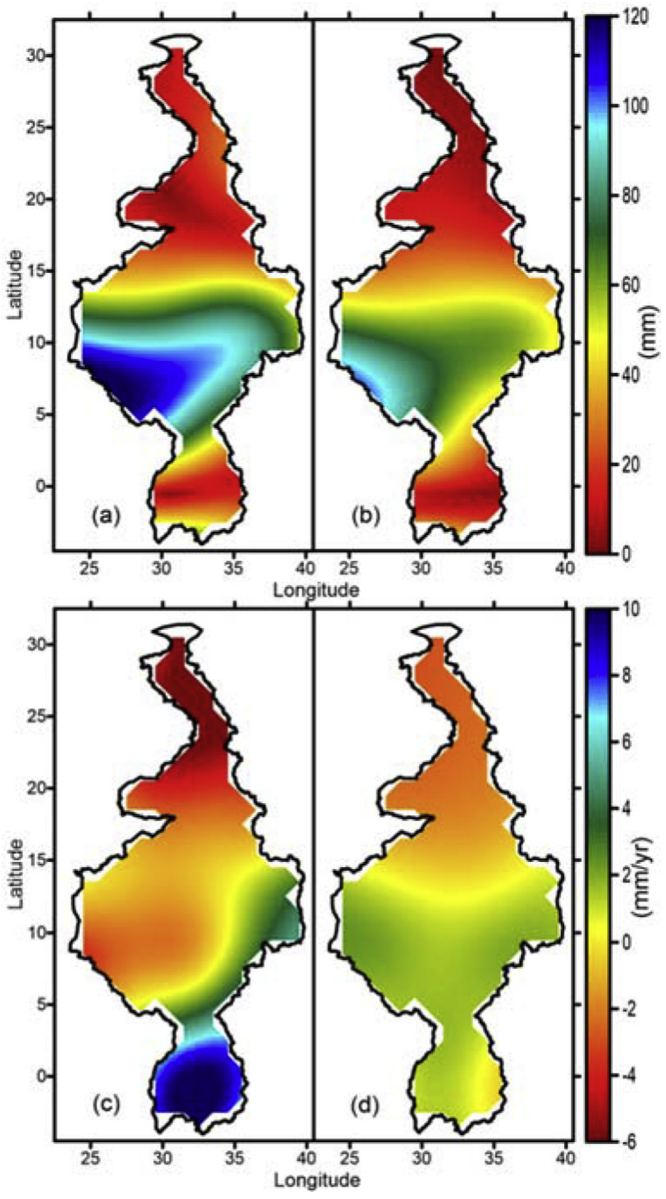

Fig. 2. Annual amplitude variations of TWS in Nile River Basin from (a) GRACE (b) GLDAS-NOAH1.0 and trend of TWS from (c) GRACE (d) GLDAS-NOAH1.0.

2.3. Temperature data

Surface temperature is used from GLDAS; NOAH model with a spatial resolution 1.0° × 1.0° is used in this research. The surface temperature is used to understand the relation between climate change and the hydrological components.

2.4. Precipitation data

Tropical Rainfall Measurement Mission (TRMM) data [26], has used in this study to understand the climate change in the NRB. TRMM satellite was launched in 1997; the Tropical Rainfall Measuring Mission is a joint mission between the National Aeronautics and Space Administration (NASA) of the United States and the National Space Development Agency (NASDA) of Japan. The main objective of TRMM is to measure rainfall of tropical and subtropical regions of the world. TRMM contain the observations of

radiances, microwave temperature, radar reflectivity, rainfall rate, vertical rainfall profile, and convective and stratiform heating. TRMM is designed to cover the latitude from 50ºN to 50ºS to allow covering inaccessible areas, such as oceans and un-sampled terrains.

TRMM 3B43 dataset is used in this research; it contains the monthly data with a spatial resolution of 0.25º x 0.25º. TRMM 3B43 data resolution needs to change from 0.25º to 1.0º. The averaged method is used for re-sampling the data from 0.25º to 1.0º by using the neighbor values (the average of 16 points). Therefore, TRMM data will be in same resolution 1.0º × 1.0º as TWS from GRACE and GLDAS. Average monthly precipitation of TRMM in the NRB is from January, 2003 to August, 2016. Also, the monthly time series of TWS from GRACE and GLDAS are shown in Fig. 3.

2.5. Drought index

Drought is defined as a lack of water [27]. Drought index is a measure of the anomalies of available water with regard to long-term statistics. Drought index is computed based on the station as well as on grid data, such as precipitation, temperature, wind speed, radiation, evaporation, and soil moisture or groundwater level [28]. Drought is classified into moderate, severe, and extreme drought [29]. One of the most frequently utilized drought indexes is the Palmer Drought Severity Index (PDSI). It is based on several empirical relationships. The strength of the PDSI lies in its high level of standardization. In this paper, the Self-calibrated PDSI (Sc-PDSI) has used to understand the variations on the TWS. Sc-PDSI is developed to avoid the above-mentioned empirical relationships. Nevertheless, the number of necessary input data was not reduced [30].

3. Results and analysis

GRACE gives better results than that from GLDAS to detect the interannual variation in water storage [2,3,31]. The seasonal and secular changes of TWS in the NRB are studied from GRACE. Furthermore, the effects of precipitation, soil moisture, and drought index on TWS variations in the NRB are analyzed by relationships.

The TWS variations from GRACE in the NRB show an increasing trend in the study period from January 2003 till August 2016, with a slight increase of 0.04 mm/yr. Also, the TWS variations from GLDAS for the same period show an increasing trend of 0.14 mm/yr. The correlation coefficient between TWS from GRACE and TWS from GLDAS is 0.94. From GRACE data analysis, the maximum positive anomaly of TWS is 81.09 mm and occurred in September 2007, while the minimum negative anomaly is 66.10 mm and it happened in April 2011.

The average value for each month from the year has computed. e.g., January value calculated from all January months (2003–2016) by taking the average. Thus, the seasonal value has calculated with the same method by using the average monthly value for each month. Also, to enhance the understanding of dry and wet months, precipitation anomaly has calculated by subtracting the rainfall value from the mean value of each point [32]. Hence, the determining of places which there is an abundance or deficit in the rainfall is easier. The maximum of rainfall change occurs in the summer season (June–August) and its effect is clear on the water storage in the autumn season (September–November). While the minimum of rainfall change occurs in the winter season (December–February) and the change of the water storage is obvious in the spring season (March–May). It has observed that the change in water storage was noticeable in the following season to change of the precipitation. TWS variations show that the change during the autumn season (September–November) is larger than the change in the spring season (March–May). Average monthly value of each month in the year in the NRB of TWS changes and the precipitation variations show that the positive difference for a half of the year, Whereas TWS change, happens from the end of June till the end of December. Also, the rainfall variation occurs from the mid of April till the end of September. It is clear to see that the peak of precipitation has happened in July–August, while, the effect of the precipitation

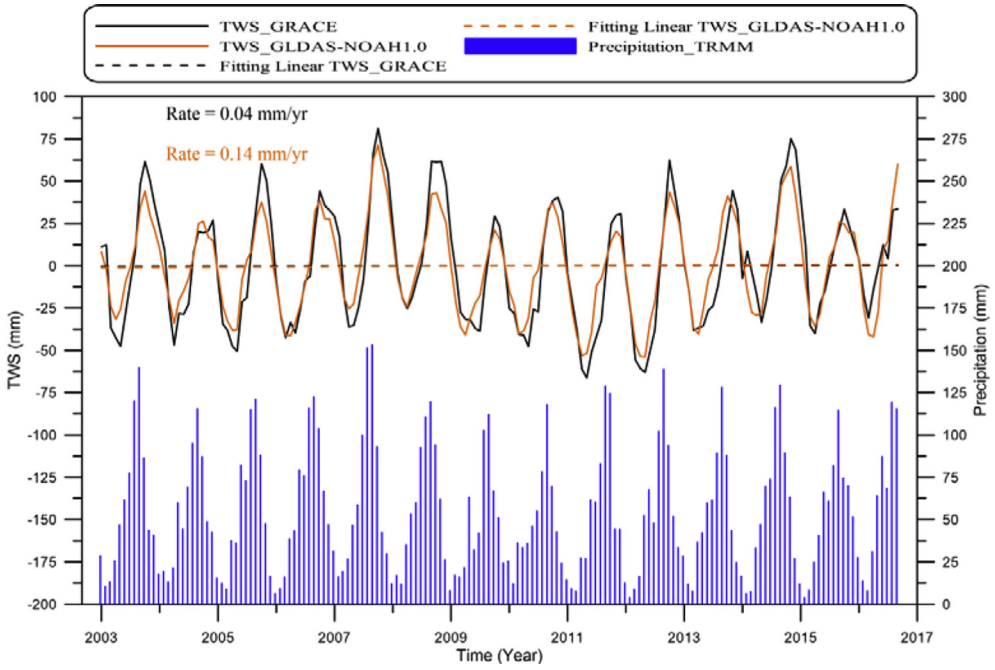

Fig. 3. Time series of average TWS and precipitation over Nile River basin.

has occurred after two months in TWS whereas the peak of TWS has appeared in September and October (Fig. 4).

The average seasonal variation in the NRB is shown in Fig. 5. The main change of the terrestrial water storage in the NRB happens in the middle of the region. The maximum variation occurs in the autumn season (SON) while the minimum variation happens in the spring season (MAM). The soil moisture variation is computed after removing the average value for each point. It is clear to see that the significant variation occurs in the same region as a TWS. The maximum and the minimum value occur in the autumn season (SON) and spring season (MAM), respectively.

Also, the most precipitation variations happen in the middle region of the NRB. The maximum and the minimum value occur in the same area as a Lake Tana (The east of the middle region). Also in the south of the region especially in the Lake Victoria location, the precipitation variation appears clearly, but in the different seasons.

As mentioned above, the effect of rainfall on the water storage has shown in the following season. While the effect of rainfall on the soil moisture is clear in the same season but it is more apparent in the following season.

4. Discussion

The average of TWS for each latitude is computed for every month of the study period. Also for each longitude, the average of TWS for each month is calculated. Spatial distribution of TWS from GRACE show notable gradients of decreasing TWS from south to north and from west to east in Fig. 6, which are likely to be associated with the impact of monsoons and topography [33–35]. The average TWS over each longitudinal zone and latitudinal zone have computed in the NRB from during the study period.

The NRB is based on two main sources of water; the first source is a Lake Tana (85%) and located in the east of the middle region, and the second source is a Lake Victoria (15%) and lies in the southern region. Rainfall time varied in each of the two sources. Fig. 6 can refer to understand the flood and drought in the NRB. For instance, severe drought occurs from 2004 through 2006, 2010, 2011, and 2012. However, the most severe droughts occurred in 2006 and 2011.

For more understanding of drought times in the NRB, the average monthly time series of TWS, ScPDSI, and non-seasonal TWS are shown in Fig. 7. Non-seasonal TWS has computed by subtracting the monthly average value of TWS from the seasonal cycle value. Whereas the seasonal cycle computes by:

$$y = A\cos(\omega t + \phi) \tag{8}$$

where A is amplitude, ω is frequency, and ϕ is phase. The correlation factor between the non-seasonal TWS and ScPDSI is 0.60, indicating that GRACE-derived TWS well capture the most severe droughts occurred in 2006 and 2011 [36].

The correlation coefficients between TWS variations, precipitation, and temperature computed from the monthly data. TWS shows a weak correlated with rainfall and temperature at same month in the NRB region with a correlation of 0.43 and −0.18 respectively. On the other hand, the shifted TWS (two months shifted) shows a strong correlation with rainfall with a correlation of 0.87, while the correlation is 0.51 with a temperature. The soil moisture is a highly correlated with TWS at a correlation of 0.88 (Table 1).

Also, the correlation coefficients between precipitation and TWS variation and shifted TWS (shifted two months) have computed in Fig. 8. The spatial Spearman correlation distribution has shown that the range of correlation between −0.37 and 0.57 with an average of 0.25 and $p < 0.05$ in Fig. 8a. While the range of correlation between −0.20 and 0.88 with an average of 0.53 and $p < 0.05$ in Fig. 8b which shows a significant correlation in the middle region of the NRB.

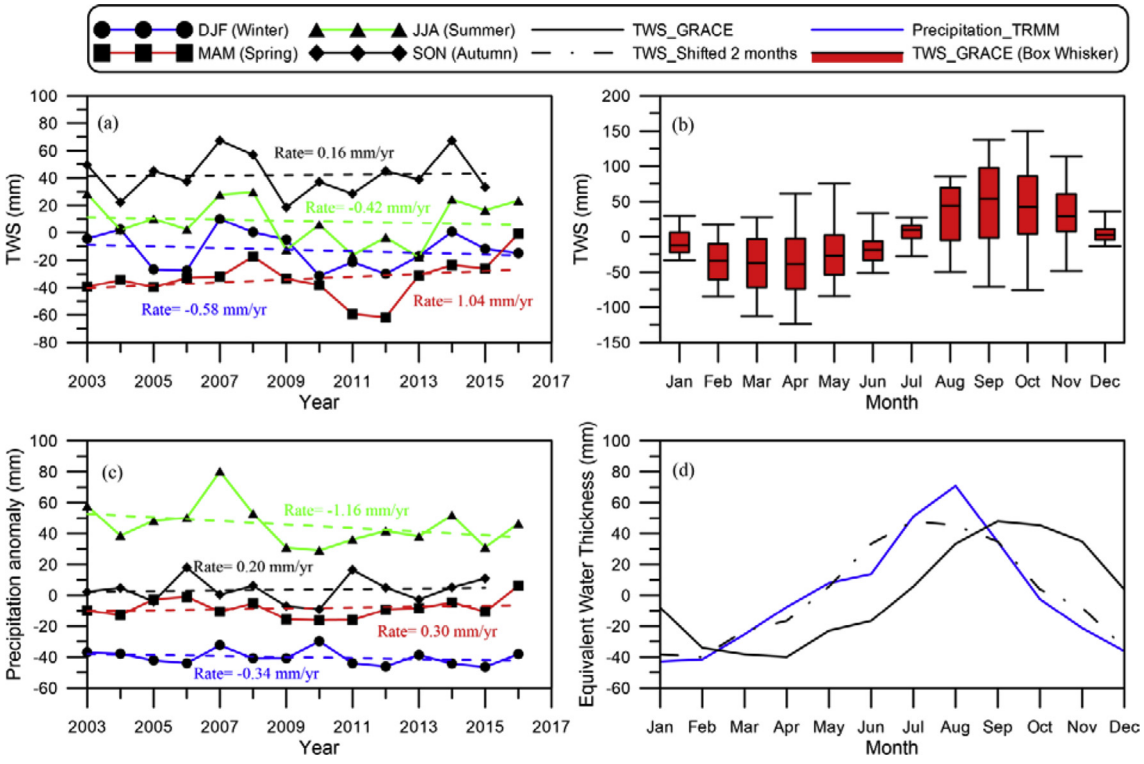

Fig. 4. Seasonal and annual variations in terrestrial water storage and precipitation in the Nile River Basin.

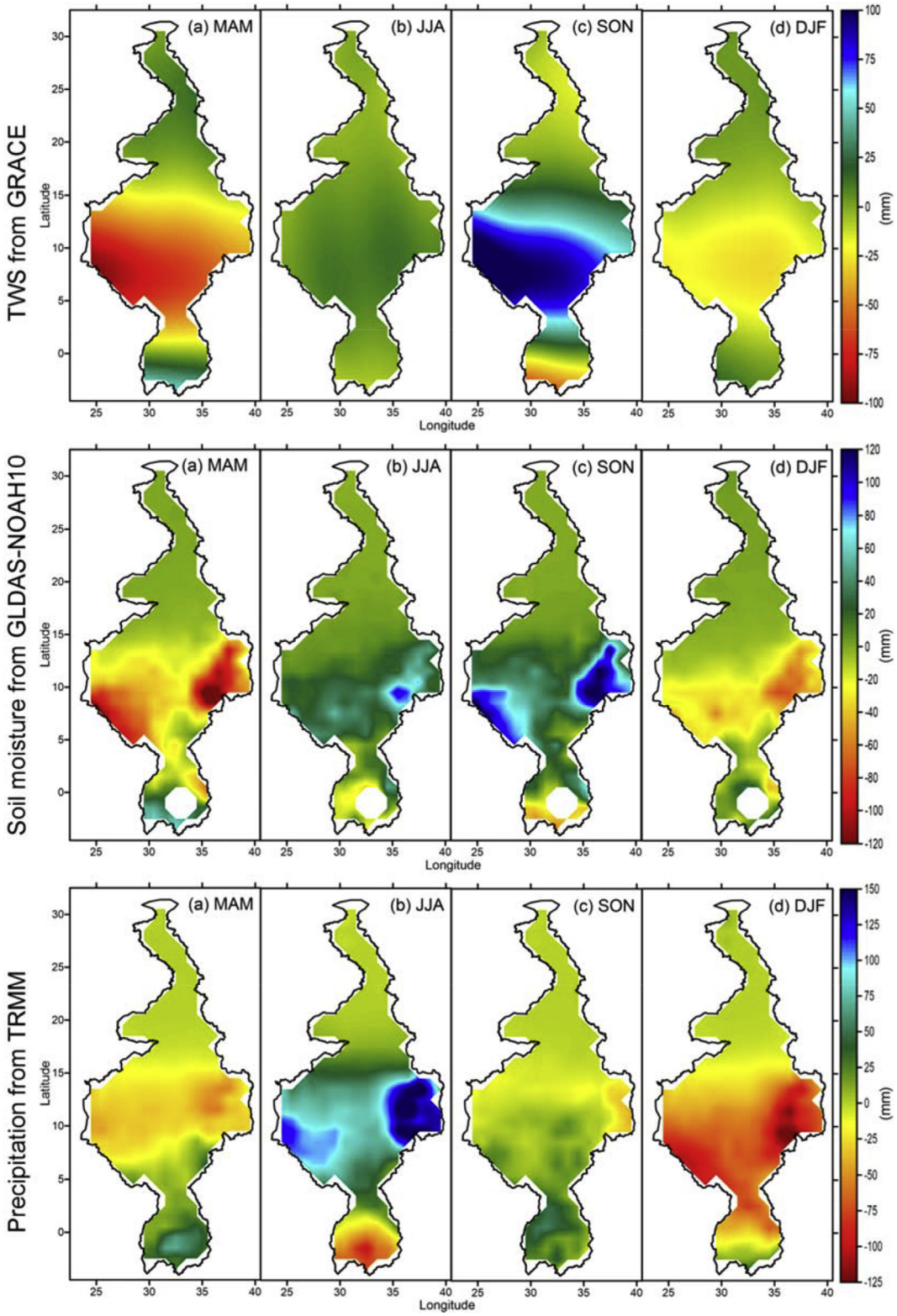

Fig. 5. Mean seasonal variations in the Nile River Basin.

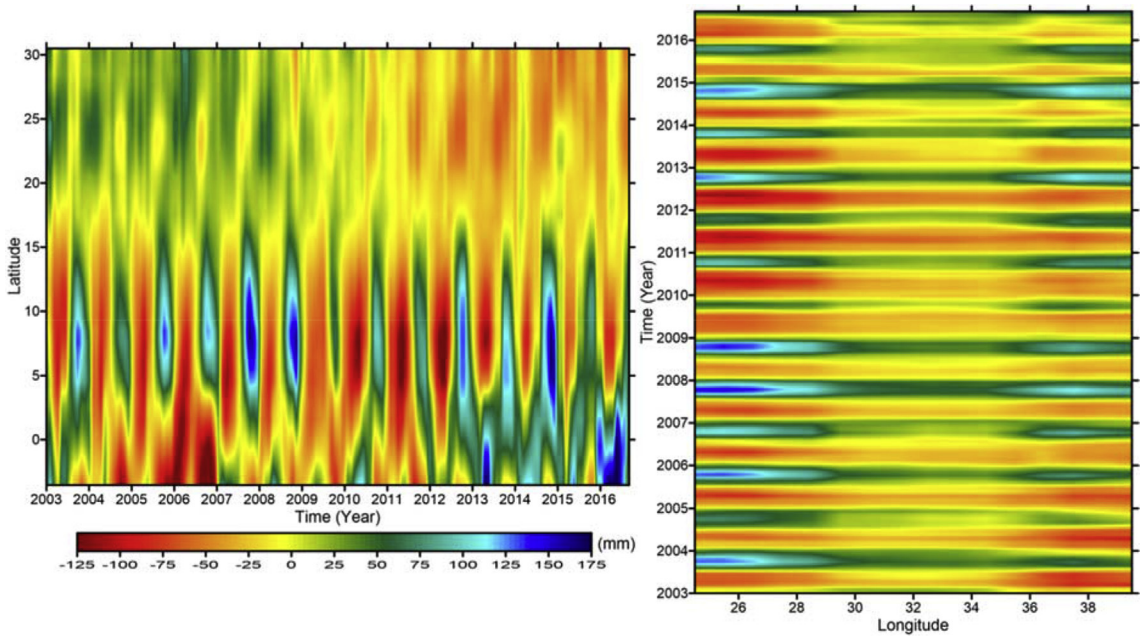

Fig. 6. Average TWS from GRACE over longitudes for each latitude (left side) and average TWS from GRACE over latitudes for each longitude (right side).

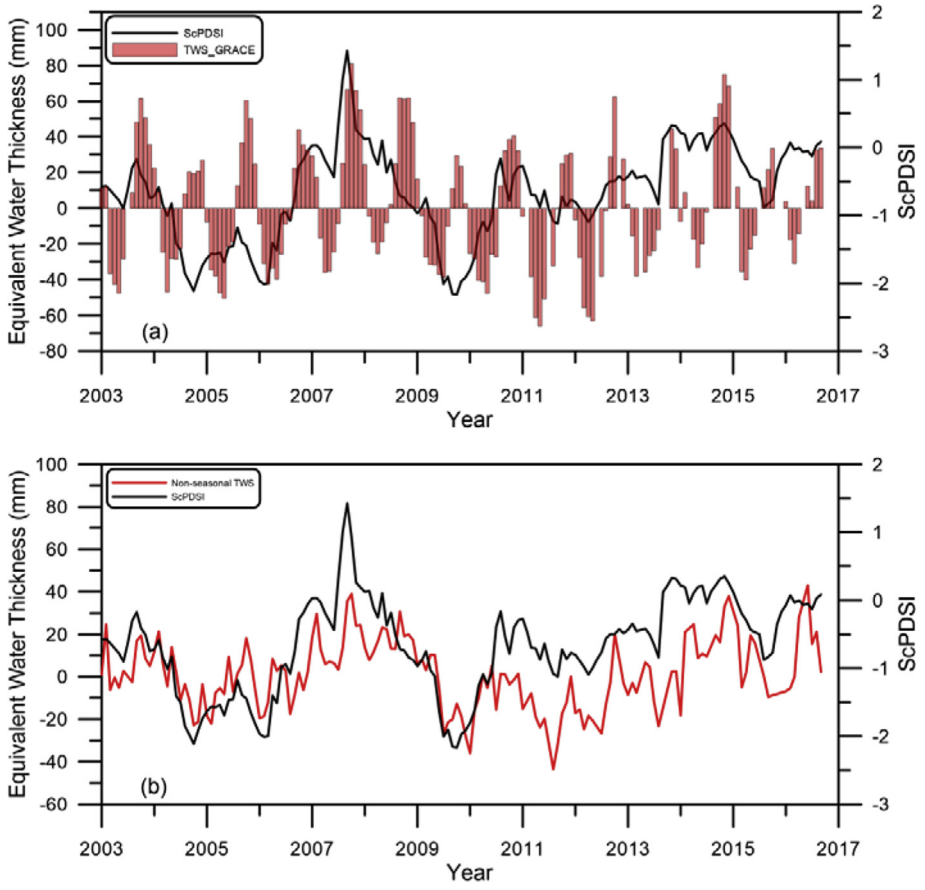

Fig. 7. Monthly variations (a) TWS and self-calibrating Palmer Drought Severity Index (ScPDSI) (b) Non-seasonal TWS and ScPDSI.

Table 1
Person correlation coefficients of the average monthly time series of TWS with precipitation, soil moisture, and temperature in the Nile River Basin.

Correlation	Terrestrial Water Storage	
	TWS	TWS with shifted 2 months
Precipitation	0.43	0.87
Soil moisture	0.88	0.63
Temperature	−0.18	0.51

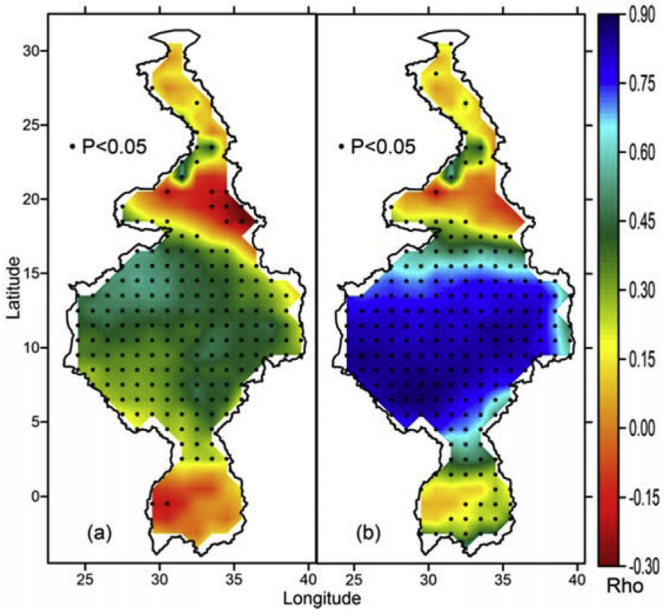

Fig. 8. Correlation between TWS and precipitation in the Nile River Basin (a) Spearman correlation between TWS and precipitation (b) Spearman correlation between shifted two months TWS and Precipitation. The black dot signs represent significant correlations at level of $P<0.05$.

5. Conclusions

In this study, the TWS is computed from GRACE and compared with the TWS from GLDAS in terms of the average monthly time series throughout the study period with the correlation coefficient of 0.94. The maximum average monthly of TWS variation from GRACE in the NRB is 81.09 mm in September 2007, and its minimum is −66.10 mm in April 2011, which coincided with the occurrence of floods and drought respectively in the NRB.

Furthermore, the effect of rainfall appears on the soil moisture at the following month, but it is clearer after two months. While the TWS changes appear with a phase lag of two months from the rainfall to coincide with the change in the soil moisture. Whereas, the maximum seasonally TWS from GRACE measurements is 42.66 mm during autumn (SON), and its minimum is −33.77 mm during spring (MAM). Also, the maximum seasonally soil moisture is 25.22 mm during autumn (SON), and its minimum is −23.34 mm during spring (MAM) while the peak seasonally precipitation is 100.11 mm during summer (JJA) and its minimum is 14.62 mm during winter (DJF). The trend of TWS is a slight increase in the NRB with 0.04 mm/yr.

The upper region is arid. In addition, the precipitation is rare. The middle region of the NRB is the most influential where the Lake Tana is located. Also, the south region especially in the Lake Victoria location, the precipitation variation appears clearly but in the different season (spring, MAM). In addition, the correlation factor between the non-seasonal TWS and ScPDSI is 0.60, indicating that GRACE-derived TWS can well capture the most severe droughts occurred in 2006 and 2011.

Conflicts of interest

The authors declare that there is no conflicts of interest. The founding sponsors had no role in the design of the study; in the collection, analyses, or interpretation of data; in the writing of the manuscript, and in the decision to publish the results.

Acknowledgments

This work was supported by the National Natural Science Foundation of China (Grant No. 11373059) and sponsored by CAS-TWAS President's Fellowship for International PhD Students.

References

[1] H. Deng, Y. Chen, Influences of recent climate change and human activities on water storage variations in Central Asia, J. Hydrol. 544 (Suppl. C) (2017) 46–57, https://doi.org/10.1016/j.jhydrol.2016.11.006.
[2] A. Hassan, S. Jin, Water cycle and climate signals in Africa observed by satellite gravimetry, IOP Conf. Ser. Earth Environ. Sci. 17 (1) (2014) 012149.
[3] T.H. Syed, et al., Analysis of terrestrial water storage changes from GRACE and GLDAS, Water Resour. Res. 44 (2) (2008), https://doi.org/10.1029/2006WR005779 n/a-n/a.
[4] N. Tangdamrongsub, et al., Data assimilation of GRACE terrestrial water storage estimates into a regional hydrological model of the Rhine River basin, Hydrol. Earth Syst. Sci. 19 (4) (2015) 2079–2100, https://doi.org/10.5194/hess-19-2079-2015.
[5] J. Awange, et al., Frequency and severity of drought in the Lake Victoria region (Kenya) and its effects on food security, Clim. Res. 33 (2) (2007) 135–142, https://doi.org/10.3354/cr033135.
[6] A. Hassan, S. Jin, Water storage changes and balances in Africa observed by GRACE and hydrologic models, Geodesy and Geodynamics 7 (1) (2016) 39–49, https://doi.org/10.1016/j.geog.2016.03.002.
[7] J.W. Crowley, et al., Land water storage within the Congo Basin inferred from GRACE satellite gravity data, Geophys. Res. Lett. 33 (19) (2006), https://doi.org/10.1029/2006GL027070.
[8] A.C. Thomas, et al., A GRACE-based water storage deficit approach for hydrological drought characterization, Geophys. Res. Lett. 41 (5) (2014) 1537–1545, https://doi.org/10.1002/2014GL059323.
[9] A.M. Melesse, W. Abtew, S.G. Setegn, Nile River Basin, Springer, 2011, https://doi.org/10.1007/978-94-007-0689-7.
[10] J. Wahr, et al., Time-variable gravity from GRACE: first results, Geophys. Res. Lett. 31 (11) (2004), https://doi.org/10.1029/2004GL019779.
[11] S. Jin, G. Feng, Large-scale variations of global groundwater from satellite gravimetry and hydrological models, 2002–2012, Glob. Planet. Chang. 106 (2013) 20–30, https://doi.org/10.1016/j.gloplacha.2013.02.008.
[12] A. Hassan, S. Jin, Lake level change and total water discharge in East Africa Rift Valley from satellite-based observations, Glob. Planet. Chang. 117 (2014b) 79–90, https://doi.org/10.1016/j.gloplacha.2014.03.005.
[13] M. Shamsudduha, et al., Recent changes in terrestrial water storage in the Upper Nile Basin: an evaluation of commonly used gridded GRACE products, Hydrol. Earth Syst. Sci. 21 (9) (2017) 4533–4549, https://doi.org/10.5194/hess-21-4533-2017.
[14] L. Longuevergne, et al., GRACE water storage estimates for the Middle East and other regions with significant reservoir and lake storage, Hydrol. Earth Syst. Sci. 17 (12) (2013) 4817–4830, https://doi.org/10.5194/hess-17-4817-2013.
[15] S. Swenson, J. Wahr, Post-processing removal of correlated errors in GRACE data, Geophys. Res. Lett. 33 (8) (2006), https://doi.org/10.1029/2005GL025285.
[16] J.L. Chen, et al., Recent La Plata basin drought conditions observed by satellite gravimetry, J. Geophys. Res.: Atmospheres 115 (D22) (2010), https://doi.org/10.1029/2010JD014689.
[17] S. Jin, A. Hassan, G. Feng, Assessment of terrestrial water contributions to polar motion from GRACE and hydrological models, J. Geodyn. 62 (2012) 40–48, https://doi.org/10.1016/j.jog.2012.01.009.
[18] B.D. Tapley, et al., The gravity recovery and climate experiment: mission overview and early results, Geophys. Res. Lett. 31 (9) (2004b), https://doi.org/10.1029/2004GL019920.
[19] M. Cheng, B.D. Tapley, Variations in the Earth's oblateness during the past 28 years, J. Geophys. Res.: Solid Earth 109 (B9) (2004), https://doi.org/10.1029/2004JB003028.
[20] S. Swenson, D. Chambers, J. Wahr, Estimating geocenter variations from a combination of GRACE and ocean model output, J. Geophys. Res.: Solid Earth 113 (B8) (2008), https://doi.org/10.1029/2007JB005338 n/a-n/a.
[21] J. Wahr, M. Molenaar, F. Bryan, Time variability of the Earth's gravity field: hydrological and oceanic effects and their possible detection using GRACE,

J. Geophys. Res.: Solid Earth 103 (B12) (1998) 30205–30229, https://doi.org/10.1029/98JB02844.
[22] M.B. Ek, et al., Implementation of Noah land surface model advances in the National Centers for Environmental Prediction operational mesoscale Eta model, J. Geophys. Res.: Atmospheres 108 (D22) (2003), https://doi.org/10.1029/2002JD003296.
[23] H. Fang, et al., Global Land Data Assimilation System (GLDAS) Products from NASA Hydrology Data and Information servIces Center (HDISC), in ASPRS, 2008. Portland, Oregon.
[24] B. Hofmann-Wellenhof, H. Moritz, Physical Geodesy, 2nd., Springer Wien NewYork, Austria, 2006 https://doi.org/10.1007/978-3-211-33545-1.
[25] H. Abd-Elmotaal, et al., Comparison among three harmonic analysis techniques on the sphere and the ellipsoid, J. Appl. Geod. 8 (1) (2014) 1–20, https://doi.org/10.1515/jag-2013-0008.
[26] G.J. Huffman, et al., The TRMM multisatellite precipitation analysis (TMPA): Quasi-global, multiyear, combined-sensor precipitation estimates at fine scales, J. Hydrometeorol. 8 (1) (2007) 38–55, https://doi.org/10.1175/jhm560.1.
[27] R.R. Heim, A review of twentieth-century drought indices used in the United States, Bull. Am. Meteorol. Soc. 83 (8) (2002) 1149–1165, https://doi.org/10.1175/1520-0477(2002)083<1149:arotdi>2.3.co;2.
[28] M. Ziese, et al., The GPCC Drought Index – a new, combined and gridded global drought index, Earth Syst. Sci. Data 6 (2) (2014) 285–295, https://doi.org/10.5194/essd-6-285-2014.
[29] W. Palmer, Meteorological drought, Research paper no.45 1965 [cited 2017 6 December]; Research paper no.45]. Available from: http://www.ncdc.noaa.gov/temp-and-precip/drought/docs/palmer.pdf.
[30] N. Wells, S. Goddard, M.J. Hayes, A self-calibrating Palmer drought severity index, J. Clim. 17 (12) (2004) 2335–2351, https://doi.org/10.1175/1520-0442(2004)017<2335:aspdsi>2.0.co;2.
[31] T. Yang, et al., Characterization of spatio-temporal patterns for various GRACE- and GLDAS-born estimates for changes of global terrestrial water storage, Glob. Planet. Chang. 109 (2013) 30–37, https://doi.org/10.1016/j.gloplacha.2013.07.005.
[32] C. Tocho, et al., Seasonal variability of land water storage in south America using GRACE data, in: M.C. Pacino, U. Marti (Eds.), Geodesy for Planet Earth: Proceedings of the 2009 IAG Symposium, Buenos Aires, Argentina, 31 August 31 - 4 September 2009, S. Kenyon, Springer Berlin Heidelberg, Berlin, Heidelberg, 2012, pp. 605–611.
[33] A. Asoka, et al., Relative contribution of monsoon precipitation and pumping to changes in groundwater storage in India, Nat. Geosci. 10 (2017) 109, https://doi.org/10.1038/ngeo2869. https://www.nature.com/articles/ngeo2869#supplementary-information.
[34] T. Phillips, et al., The influence of ENSO on global terrestrial water storage using GRACE, Geophys. Res. Lett. 39 (16) (2012), https://doi.org/10.1029/2012GL052495.
[35] Z. Zhang, et al., Terrestrial water storage anomalies of Yangtze River Basin droughts observed by GRACE and connections with ENSO, Glob. Planet. Chang. 126 (2015) 35–45, https://doi.org/10.1016/j.gloplacha.2015.01.002.
[36] S. Jin, T. Zhang, Terrestrial water storage anomalies associated with drought in Southwestern USA from GPS observations, Surv. Geophys. 37 (6) (2016) 1139–1156, https://doi.org/10.1007/s10712-016-9385-z.

Mostafa Abd-Elbaky is an assistant professor at the faculty of Engineering, Minia University, Egypt. He has finished his M.Sc. in geodesy from Minia University. Also, he got his Ph.D. degree from Shanghai Astronomical Observatory, Chinese Academy of Sciences, China. His research interests include Satellite Gravimetry and Gravity Field, Space Geodesy and Hydrologic Cycle.